

## **A STUDY OF THE EFFECT OF CALCINATION TEMPERATURE ON THE INTERACTION BETWEEN THE ACTIVE COMPONENT AND THE CARRIER OF A CATALYST USING THERMOANALYSIS AND X-RAY DIFFRACTION**

LIU JINXIANG and YANG LIXIN

*Dalian Institute of Chemical Physics, Academia Sinica, Dalian (People's Republic of China)*

JIANG XUANZHEN

*Department of Chemistry, Zhejiang University, Hangzhou (People's Republic of China)*

(Received 25 May 1990)

### **ABSTRACT**

The reduction behaviour under hydrogen of nickel catalysts supported on  $\text{Al}_2\text{O}_3$ ,  $\text{Nb}_2\text{O}_5$ ,  $\text{TiO}_2$  and ground glass carriers has been studied by thermoanalysis. The results show that the active component, NiO, interacts with  $\text{Nb}_2\text{O}_5$  to form  $\text{NiNb}_2\text{O}_6$  at  $400^\circ\text{C}$ , and at  $900^\circ\text{C}$  NiO interacts with  $\text{Al}_2\text{O}_3$  and  $\text{TiO}_2$  to form  $\text{NiAl}_2\text{O}_4$  and  $\text{NiTiO}_3$  respectively. The existence of the above-mentioned Support–Metal Strong Interaction (SMSI) was verified by in situ X-ray diffraction analysis. In the case of NiO/glass calcined at  $900^\circ\text{C}$  a new phase was formed; its composition has yet to be determined.

### **INTRODUCTION**

The effective surface of the metal component of a catalyst can be increased by dispersing it on a support, this being regarded as an inert substance [1,2]. Numerous experiments have shown, however, that the support is not inert. The metal component and the support interact and even form some new compounds. In 1978 Tauster and coworkers [3–5] found that the adsorption capacities for  $\text{H}_2$  and CO of Ru, Rh, Pd, Os, Ir and Pt supported on  $\text{TiO}_2$  treated with hydrogen at high temperature are much lower than when treated at low temperature. According to traditional theories, the sintering of metal at high temperature may cause the decrease in adsorbability, but neither crystal growth nor sintering have been found by X-ray diffraction analysis. Thus, the concept of Support–Metal Strong Interaction (SMSI) was proposed to explain the above-mentioned phenomena. Because of the SMSI, the catalysts have different catalytic properties [6–14], which, in particular, has an important effect on the behaviour of redox-type catalytic reactions. Thus, studies of SMSIs are of undoubtedly

important and wide ranging significance in the understanding of catalysts and catalysis, and in enhancing the catalytic properties of catalysts by modifying the SMSIs.

In recent years, SMSI study has achieved further development following the application of modern physical measurement techniques. Numerous investigations have shown that SMSI depends not only on the metal and support themselves, but also on the dispersion of the metal and on the catalyst preparation conditions, such as calcination temperature and reduction. In this work, starting with the calcination of catalysts, we have studied the reduction behaviour of nickel catalysts supported on  $\text{Al}_2\text{O}_3$ ,  $\text{Nb}_2\text{O}_5$ ,  $\text{TiO}_2$  and ground glass carriers using thermoanalysis to delineate the mechanism of SMSI. In addition, the existence of SMSI was verified by in situ X-ray diffraction. Some valuable information concerning the improvement of nickel catalysts has also been obtained.

## EXPERIMENTAL

### *Catalyst samples*

The catalysts investigated were 9% NiO/ $\text{Al}_2\text{O}_3$ , 12.5% NiO/ $\text{Nb}_2\text{O}_5$ , 13% NiO/ $\text{TiO}_2$  and 3.8% NiO/glass.

### *Apparatus and requirements*

The calcination and reduction of the catalysts were carried out on an attached TG-DTG unit of a Shimadzu DT-20B type thermoanalyser with the following experimental conditions: measuring range, 2–10 mg; heating rate,  $10^\circ\text{C min}^{-1}$ ; and paper speed,  $1.25\text{ mm min}^{-1}$ .

XRD analysis was carried out on a Rigaku D/max IIIB X-ray diffractometer: Cu  $K\alpha$ , 40 kV, 50 mA (Ni filter), scanning rate  $2\text{ deg min}^{-1}$ .

## RESULTS AND DISCUSSION

### *Reduction of calcined NiO/ $\text{Al}_2\text{O}_3$ under $\text{H}_2$*

TG-DTG curves of NiO/ $\text{Al}_2\text{O}_3$  calcined at 400 and  $900^\circ\text{C}$  and reduced in  $\text{H}_2$  are given in Fig. 1; their X-ray diffraction patterns are shown in Fig. 2.

Figure 1 shows that two peaks appear in the DTG curve of NiO/ $\text{Al}_2\text{O}_3$  calcined at  $400^\circ\text{C}$ , the relevant weight loss being observed in the corresponding TG curve. The first peak is the desorption of  $\text{H}_2\text{O}$  from the surface. The second peak is in the range  $320\text{--}640^\circ\text{C}$  with a peak tempera-

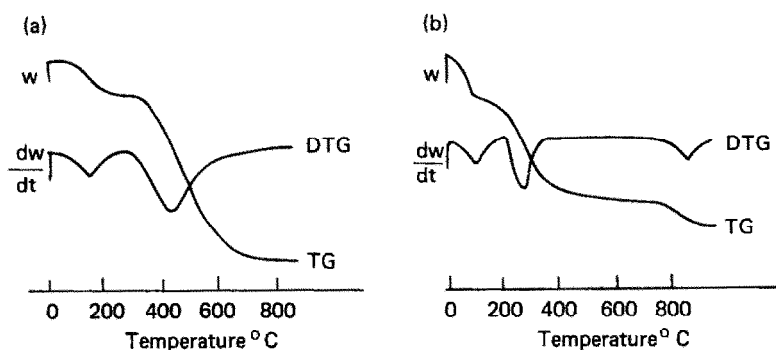


Fig. 1. TG-DTG curves of NiO/Al<sub>2</sub>O<sub>3</sub> catalyst reduced by H<sub>2</sub>: (a), sample calcined at 400 °C; (b), sample calcined at 900 °C.

ture of 430 °C and shows the reduction of NiO. In comparison with the reduction of single component NiO, the temperature range of the reduction has shifted backwards and the weight loss far exceeds the theoretical. This is due to the weight loss of NiO by reduction and also the loss of hydroxyl group on Al<sub>2</sub>O<sub>3</sub>. There is no obvious change in the TG-DTG curve above 640 °C.

XRD patterns reveal the presence of a very fine NiAl<sub>2</sub>O<sub>4</sub> crystal phase but the diffraction peak is diffuse, demonstrating that only a little active metal component forms NiAl<sub>2</sub>O<sub>4</sub> with Al<sub>2</sub>O<sub>3</sub>, and that most of the active component is still in the form of NiO.

Three peaks appear in the DTG curve of NiO/Al<sub>2</sub>O<sub>3</sub> calcined at 900 °C, the corresponding TG curves showing the relevant weight loss. The first peak indicates the desorption of surface water; the second is in the range 205–340 °C, with the peak at 260 °C, indicating the reduction of NiO; the third occurs over the range 742–950 °C with the peak at 846 °C and is

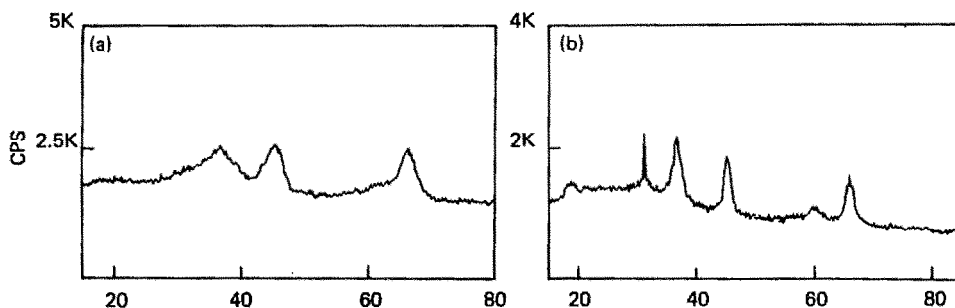


Fig. 2. XRD patterns of NiO/Al<sub>2</sub>O<sub>3</sub> catalyst: (a), sample calcined at 400 °C; (b), sample calcined at 900 °C.

TABLE 1

Ni content of NiO/Al<sub>2</sub>O<sub>3</sub> determined by thermogravimetry and chemical analysis

Reaction	Weight loss (mg)	Ni content (mg)	Ni (%)		
			TG	Total	Chemical analysis
Reduction of NiO	0.298	1.09	5.2	8.4	9
Reduction of NiAl <sub>2</sub> O <sub>4</sub>	0.298	0.667	3.2		

Sample weight 20.77 mg.

expected to represent the reduction of NiO · Al<sub>2</sub>O<sub>3</sub> (the SMSI product of NiO and Al<sub>2</sub>O<sub>3</sub>). The reduction reactions are



and the Ni content calculated from the weight loss by reduction is compared with the results of chemical analyses in Table 1. It can be seen that the total Ni content calculated from the weight loss of NiO and NiAl<sub>2</sub>O<sub>4</sub> by reduction is basically consistent with the analytical result; thus, the third peak can be assigned as the reduction of NiAl<sub>2</sub>O<sub>4</sub>.

XRD patterns show that NiAl<sub>2</sub>O<sub>4</sub> is the main phase, demonstrating that most of the active component, NiO, and Al<sub>2</sub>O<sub>3</sub> carrier form a new spinel compound, nickel aluminate, through SMSI.

#### Reduction of calcined NiO/Nb<sub>2</sub>O<sub>5</sub> under H<sub>2</sub>

TG-DTG curves of NiO/Nb<sub>2</sub>O<sub>5</sub> (calcined at 450 and 900 °C) reduced in H<sub>2</sub> are shown in Fig. 3 and their XRD patterns are illustrated in Fig. 4. There are two peaks in the DTG curve (Fig. 3) of the NiO/Nb<sub>2</sub>O<sub>5</sub> catalyst calcined at 450 °C, with no peak for NiO reduction: The first is the

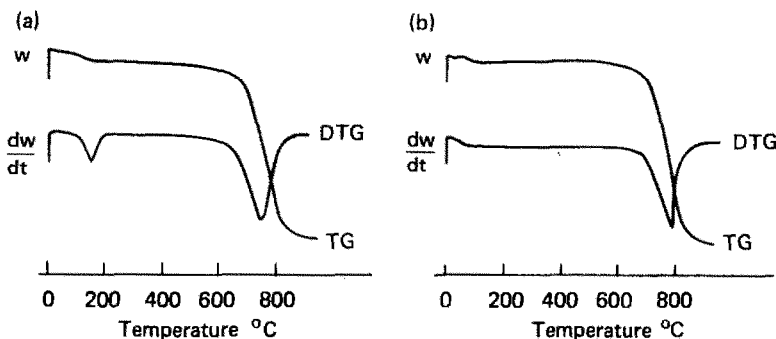


Fig. 3. TG-DTG curves of NiO/Nb<sub>2</sub>O<sub>5</sub> catalyst reduced by H<sub>2</sub>: (a), sample calcined at 450 °C; (b), sample calcined at 900 °C.

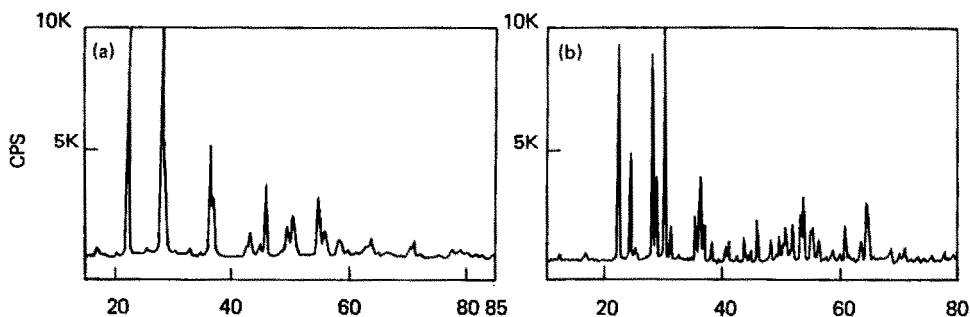
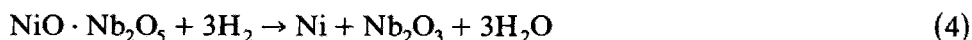
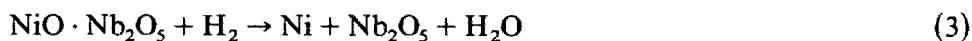


Fig. 4. XRD patterns of NiO/Nb<sub>2</sub>O<sub>5</sub> catalyst: (a), sample calcined at 450 °C; (b), sample calcined at 900 °C.

desorption of surface water; the second, in the range 623–810 °C with the peak at 775 °C, may be the reduction of NiO · Nb<sub>2</sub>O<sub>5</sub> (the product of NiO and Nb<sub>2</sub>O<sub>5</sub> via SMSI). Assuming the reduction of NiO · Nb<sub>2</sub>O<sub>5</sub> is as follows



the Ni content calculated from weight loss by reduction is compared with the results of chemical analysis in Table 2. The results calculated according to reactions (3) and (4) are not in agreement with those obtained by chemical analysis; this may be because the supposed reduction product is not rational.

The XRD patterns show the presence of an NiNb<sub>2</sub>O<sub>6</sub> phase, the new compound formed between NiO and Nb<sub>2</sub>O<sub>5</sub> by SMSI.

In the DTG curve of the reduced sample calcined at 900 °C, there is only one peak present in the range of 650–820 °C, the peak temperature being 770 °C; the relevant weight loss is observed in the corresponding TG curve. Obviously, it is due to the reduction of the SMSI product NiO · Nb<sub>2</sub>O<sub>5</sub>. The Ni contents calculated according to reactions (3) and (4) are compared with those of the sample calcined at 450 °C in Table 3. The results show that the Ni contents calculated for the sample calcined at 900 °C are higher than for those calcined at 450 °C.

TABLE 2

Ni content of NiO/Nb<sub>2</sub>O<sub>5</sub> determined by thermogravimetry and chemical analysis

Reaction	Weight loss (mg)	Proportion of weight loss		Ni content (mg)	Ni (%)	
		NiO	Nb <sub>2</sub> O <sub>5</sub>		TG	Chemical analysis
Eqn. (3)	1.67	1	0	6.12	18.6	12.5
Eqn. (4)		1/3	2/3	2.04	6.2	

Sample weight 32.9 mg.

TABLE 3

Ni content of NiO/Nb<sub>2</sub>O<sub>5</sub> catalyst

Sample weight (mg)	Calcination temperature (°C)	Reaction	Ni content	
			(mg)	(%)
32.9	450	Eqn. (3)	6.12	18.6
		Eqn. (4)	2.04	6.2
28.2	900	Eqn. (3)	5.50	19.5
		Eqn. (4)	1.8	6.5

The same NiNb<sub>2</sub>O<sub>6</sub> phase is observed in the XRD pattern of the sample calcined at 900°C, it being present in slightly higher amounts than in the sample calcined at 450°C, showing that although NiNb<sub>2</sub>O<sub>6</sub> phase is present at 450°C, its formation is more complete at 900°C.

#### *Reduction of calcined NiO/TiO<sub>2</sub> under H<sub>2</sub>*

The TG-DTG curves of NiO/TiO<sub>2</sub> (calcined at 400 and 900°C) reduced in H<sub>2</sub> are given in Fig. 5, and their XRD patterns are shown in Fig. 6.

Figure 5 shows that there are five peaks on the DTG curve of NiO/TiO<sub>2</sub> calcined at 400°C and the relevant weight loss is observed on their corresponding TG curves. The first and second peaks appearing below 160°C show the desorption of surface water. Because the carrier is composed of two crystal types of TiO<sub>2</sub> (rutile: anatase = 30:70), there are two dehydration temperatures. The overlapping peaks (310 and 420°C) are in the range 273–560°C, which may correspond to the reduction of NiO on the two types of TiO<sub>2</sub> carrier. In order to confirm this, the total amount of Ni calculated from weight loss by reduction is compared with that determined by chemical analysis in Table 4. The calculated Ni content is slightly lower than that determined, because of the non-uniform nature of the sample, and

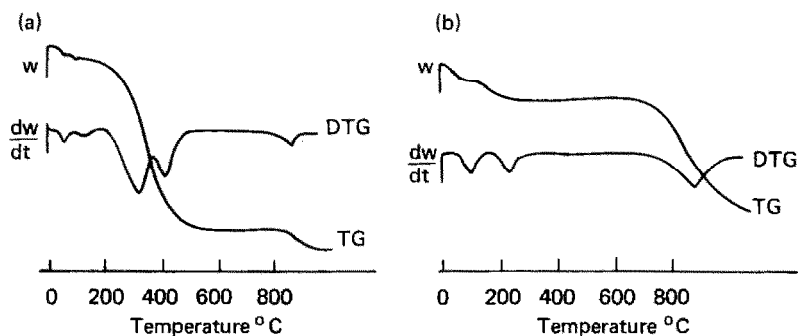


Fig. 5. TG-DTG curves of NiO/TiO<sub>2</sub> catalyst reduced by H<sub>2</sub>: (a), sample calcined at 400°C; (b), sample calcined at 900°C.

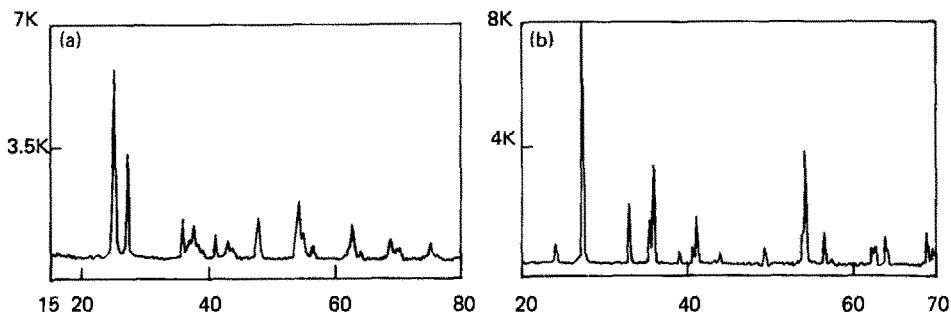


Fig. 6. XRD patterns of NiO/TiO<sub>2</sub> catalyst: (a), sample calcined at 400°C; (b), sample calcined at 900°C.

shows that the active component has not interacted with the TiO<sub>2</sub> and remains in the form of NiO. The fifth peak appears above 800°C and is assigned to the reduction of TiO<sub>2</sub> by comparison with the TG-DTG curve of single component TiO<sub>2</sub> reduced in H<sub>2</sub>.

The XRD patterns show the existence of anatase and rutile with the former predominant; there is no interaction between the active component, NiO, and the two types of TiO<sub>2</sub> carrier.

There are three peaks present in the TG-DTG curve of the reduced NiO/TiO<sub>2</sub> sample calcined at 900°C, and the relevant weight loss is seen on the corresponding TG curve. The first two peaks, below 200°C, show the desorption of surface water on the two types of TiO<sub>2</sub>; the peak temperatures are higher than those of the sample calcined at 400°C. The third peak appears above 750°C, about 50°C lower than the reduction temperature of single component TiO<sub>2</sub>, and is regarded as the reduction of NiO·TiO<sub>2</sub>, the product of the interaction of NiO with TiO<sub>2</sub>. The continual weight loss observed up to 900°C, may include the reduction of TiO<sub>2</sub>.

The XRD pattern in Fig. 6b illustrates the disappearance of the anatase phase, part of this being transformed to rutile, and the simultaneous formation of the new phase, NiTiO<sub>3</sub>, a spinel produced by the reaction of NiO with rutile.

TABLE 4

Ni content of NiO/TiO<sub>2</sub> determined by thermogravimetry and chemical analysis

Reaction	TiO <sub>2</sub>	Weight loss (mg)	Ni content (mg)	Ni(%)		
				TG	Total	Chemical analysis
Reduction of NiO	I	0.46	1.68	6.8	11.2	13
	II	0.29	1.06	4.3		

Sample weight 24.45 mg.

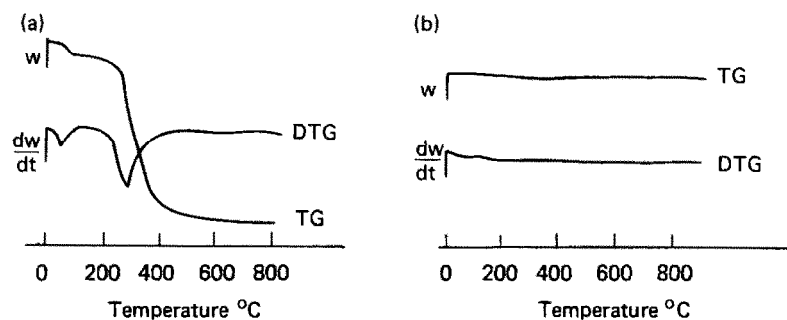


Fig. 7. TG-DTG curves of NiO/glass catalyst reduced by  $H_2$ : (a), sample calcined at  $400^\circ\text{C}$ ; (b), sample calcined at  $900^\circ\text{C}$ .

### *Reduction of calcined NiO / Glass under $H_2$*

The TG-DTG curves of NiO/glass (calcined at 400 and  $900^\circ\text{C}$ ) reduced in  $H_2$  are shown in Fig. 7, and their XRD patterns are given in Fig. 8.

There are two peaks in the DTG curve of reduced NiO/glass calcined at  $400^\circ\text{C}$  (Fig. 7), and the relevant weight loss is recorded in the corresponding TG curve. The first peak, below  $100^\circ\text{C}$  is the peak of surface water desorption. The second peak in the range  $230\text{--}335^\circ\text{C}$ , with a peak temperature of  $287^\circ\text{C}$ , shows the reduction of NiO. The calculated and determined Ni contents are compared in Table 5. Possibly because of the non-homogeneous impregnation of the catalyst, the calculated Ni content is not consistent with the determined value.

The XRD patterns show that, except for the characteristic peak of  $\text{SiO}_2$ , the remainder is NiO phase, demonstrating that no interaction takes place between NiO and the glass carrier.

There are no peaks or weight loss in the DTG-TG curves of reduced NiO/glass calcined at  $900^\circ\text{C}$ . It is possible that a new compound is formed by the reaction of NiO and glass on calcination at  $900^\circ\text{C}$  and that the new compound cannot be reduced by  $H_2$  in the temperature range from room temperature to  $900^\circ\text{C}$ , otherwise the reduction peak of NiO would appear.

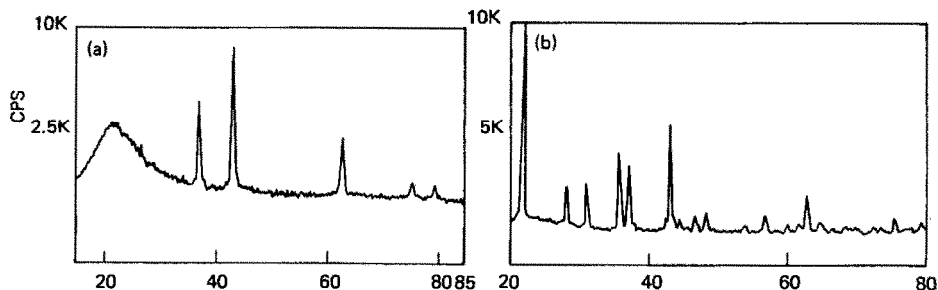


Fig. 8. XRD patterns of NiO/glass catalyst: (a), sample calcined at  $400^\circ\text{C}$ ; (b), sample calcined at  $900^\circ\text{C}$ .



TABLE 5

Ni content of NiO/glass determined by thermogravimetry and chemical analysis

Reaction	Weight loss (mg)	Ni content (mg)	Ni (%)	
			TG	Chemical analysis
Reduction of NiO	0.60	2.20	5	3.8

Sample weight 43.45 mg.

The XRD patterns show the diffraction peak of NiO, as well as a definite characteristic peak of a new phase but because of the complicated composition of the glass, its formula is unknown.

## CONCLUSION

The effect of calcination temperature on the interaction of active component and support has been studied by thermo-reduction analysis and in situ X-ray diffraction techniques. The experimental results show that the active component NiO interacted with Nb<sub>2</sub>O<sub>5</sub> carrier to form NiNb<sub>2</sub>O<sub>6</sub> when the catalyst was calcined at 400 or 450 °C. No interaction or no distinct interaction of NiO with support was observed with Al<sub>2</sub>O<sub>3</sub>, TiO<sub>2</sub> or glass. When the catalyst was calcined at 900 °C, there was interaction between NiO and Al<sub>2</sub>O<sub>3</sub> or TiO<sub>2</sub> to produce NiAl<sub>2</sub>O<sub>4</sub> or NiTiO<sub>3</sub>. Glass also interacted with NiO, but the compound formed has not yet been identified. Combined thermo-reduction analysis and in situ X-ray diffraction techniques have been shown to be an effective method in the elucidation of the interaction of metallic oxide with support.

## REFERENCES

- 1 H. Tominaga and K. Fujimoto, *Kagaku Sosetsu*, 34 (1982) 50.
- 2 I. Mochida and H. Fujitsu, *Kagaku Kogyo*, 33 (1982) 898.
- 3 S.J. Tauster, S.C. Fung and R.L. Garten, *J. Am. Chem. Soc.*, 100 (1978) 170.
- 4 S.J. Tauster and S.C. Fung, *J. Catal.*, 55 (1978) 29.
- 5 S.J. Tauster, S.C. Fung, R.T.K. Baker and J.A. Horsley, *Science*, 211 (1981) 1121.
- 6 P. Meriaudeau, H. Ellestad, and C. Naccache, *Proc. 7th Int. Congress on Catalysis*, Tokyo, 1980, Part B, pp. 1464-65.
- 7 P.G. Menon and G.F. Froment, *J. Catal.*, 59 (1979) 138.
- 8 G.J. Den Otter and F.M. Dautzenberg, *J. Catal.*, 53 (1978) 116.
- 9 M.A. Vannice and R.L. Garten, *J. Catal.*, 56 (1979) 236.
- 10 C.H. Bartholomew, R.B. Pannell and J.L. Butler, *J. Catal.*, 65 (1980) 335.
- 11 X.Z. Jiang, S.A. Stevenson and J.A. Dumesic, *J. Catal.*, 91 (1985) 11.
- 12 R. Burch and A.R. Flambard, *J. Catal.*, 78 (1982) 389.
- 13 M.A. Vannice, *J. Catal.*, 66 (1980) 242.
- 14 *J. Catal.*, 74 (1982) 199.